

Frequency Dispersion Model of the Complex Permeability of the Epoxy–Ferrite Composite

HYUNG DO CHOI,¹ KYOUNG SIK MOON,¹ IN SOO JEON,² WANG SUP KIM,² TAK JIN MOON¹

¹ Department of Materials Science, Korea University, Seoul 136-701, Republic of Korea

² Bo Sung Electric Co. Ltd. 731-2, Weonsi-Dong, Ansan-City, Kyongki-Do, Republic of Korea

Received 5 November 1996; accepted 21 April 1997

ABSTRACT: The factors that influence the complex permeability of the epoxy–ferrite composite were investigated, and the frequency dispersion behavior model for the complex permeability was proposed. The complex permeability of the composite was measured by an impedance/gain phase analyzer and a network analyzer in the frequency range from 1 MHz to 5 GHz. The permeability of the composite was increased with increasing particle size. The frequency dispersion behavior was found to be dependent on the porosity of the composite at a given particle size and ferrite content. The relaxation curve of the complex permeability became broader and flatter as the porosity increased. The equation proposed in this article coincided with the frequency dispersion behavior of the complex permeability of the composite fairly well. It was also found that the variation of σ and ν had a close relationship with the shape variation of the frequency dispersion curve, and that σ and ν were the parameters related to the porosity, particle size, and particle size distribution. © 1997 John Wiley & Sons, Inc. *J Appl Polym Sci* **66**: 477–482, 1997

Key words: epoxy–ferrite composite; complex permeability; particle size; frequency behavior

INTRODUCTION

Since polymers have the merits of lightness and good processibility, and overcame the limit of the use of sintered ferrites as the electromagnetic wave absorber, many studies on the polymer composite have been explored.^{1,2} One of those results, the polymer–ferrite composite, has been widely used as the electromagnetic wave absorber in the microwave band. The electromagnetic wave-absorbing characteristics of the absorber due to magnetic loss can be determined from composition, thickness, complex permittivity, and permeability of composite.³ Since the electromagnetic wave-absorbing properties are directly related to

the electromagnetic properties, it is of importance to analyze the electromagnetic properties of the absorber. Therefore, the modeling of the frequency dispersion behavior of the complex permeability of epoxy–ferrite composite is the substantial key to design the electromagnetic wave absorber. Accordingly, it is certain that the electromagnetic property and microwave-absorbing characteristics of the ferrite–dispersed epoxy composite depend on the variation of the composition. However, about the composites with the same filler content with different particle size, it is not easy to predict what change would occur.

In this study, the variation of the complex permeability of the composite was observed in terms of the ferrite particle size, the particle size distribution, and the porosity. The model of the frequency dispersion behavior of the composite was proposed and the experimental data were com-

Correspondence to: H. D. Choi.

Journal of Applied Polymer Science, Vol. 66, 477–482 (1997)
© 1997 John Wiley & Sons, Inc. CCC 0021-8995/97/030477-06

Table I Experimental Composition

| Raw Material | Fe ₂ O ₃ | ZnO | NiO |
|---------------|--------------------------------|-------|------|
| Ni-Zn ferrite | 66.8 | 23.83 | 9.37 |

Values are given in weight percent.

pared with the calculated value. The factors that affect the experimental variables, that is, damping and asymmetrical factor, were also investigated.

EXPERIMENTAL

The sample used in this experiment was epoxy-ferrite composite material and the polymer matrix was *o*-cresol novolac epoxy resin (ESCN 195-6, Sumitomo Chemical Co., Tokyo, Japan). As shown in Table I, Fe₂O₃, NiO, and ZnO (99%; Aldrich Chemical Co., Inc., Milwaukee, WI) were weighed, then ball-milled with ethyl alcohol for 24 h, and dried in an oven for 10 h. The dried sample was calcined in a box furnace at 1200°C for 2 h and ground for further treatment.

The obtained ferrite powder was sieved, and the average particle sizes of 88–105, 74–88, 62–74, 53–62, 44–53, and < 45 μm were obtained, respectively. To remove the agglomeration, the particles were separated five times in an ultrasonic cleaner, and then the sedimentation of the particles was performed in a glass tube (1.5 cm × 1 m). After sedimentation, a middle portion from the sedimented cake was selected. To obtain a particle of narrow size distribution, the sedimentation for one particle size was made three times. The ferrite particle size distribution was measured by a SKA-5000 particle size analyzer (Seishin Co., Osaka, Japan).

To improve the adhesion between the filler and the polymer matrix, the ferrite surface was pretreated with silane coupling agent, A-187 (γ-glycidoxypropyltrimethoxysilane, Union Carbide Inc.). The epoxy resin was previously hardened with Tamanol 758 (phenol novolac resin, Arakawa Co.). Finally, the ferrite and epoxy were mixed in the volume fraction of 0.5 : 0.5 using the cement mixer method. After compression molding into toroidal, coaxial types, samples were cured at 180°C for 5 h. The apparent density, ρ_a , and porosity of the specimen were measured by Archimedes' method. Enamel wire (0.35-mm diameter)

was uniformly wrapped around the toroidal-type specimen 20 times, and the complex permeability was calculated from inductance, L_s , and Q (μ_r'/μ_r'') measurements in the frequency range 1–40 MHz using an impedance/gain phase analyzer (HP4194A). The complex permeability of the coaxial-type specimen was measured using a coaxial air line (HP85051-60007) and a network analyzer (HP8753C) in the frequency range 50 MHz–5 GHz.⁴

RESULTS AND DISCUSSION

The average particle sizes of the ferrite after particle size analysis were 40, 75, and 100 μm. Figure 1 shows the variation of the complex permeability for the composite with the equal volume fraction of the ferrite and epoxy as a function of the particle size. In order to eliminate the effect of porosity on the electromagnetic property, the samples having < 1.23% porosity were selected. In the frequency band below 0.8 GHz, the permeability was found to decrease as the particle size decreased. The larger the particle size, the higher the permeability. Therefore, the addition of large particles increases the permeability of the composite. Above 0.8 GHz, however, the effect of the particle size on the permeability was negligible. The frequency dispersion characteristics of the complex permeability of the composites with the different particle size distribution were also studied.

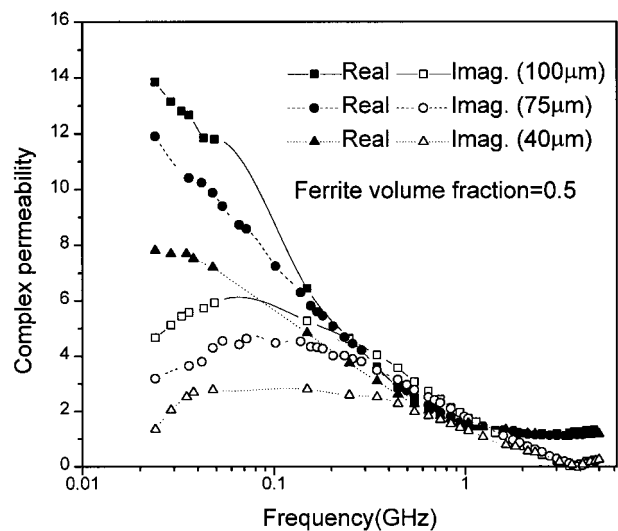


Figure 1 The dispersion spectra of complex permeability of the composite for various particle sizes of ferrite.

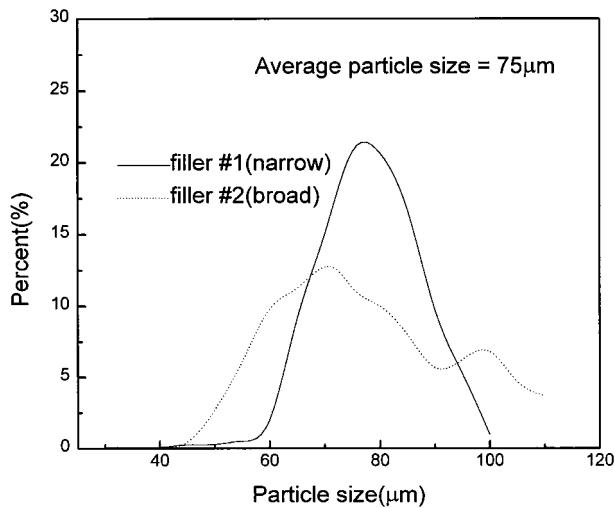


Figure 2 The particle size distribution for two types of fillers.

Figure 2 shows the particle size distributions of two types of fillers. For simplicity the narrow distributed filler was described as filler 1, the broad one as filler 2, and as can be seen, the average particle size of the both fillers was 75 μm.

Figure 3 represents the frequency dispersion behaviors of the complex permeability of the composite with filler 1 and filler 2, respectively. The density and porosity of the composites were 3.37 g/cm³, 1.15%, respectively. It was found that the composite with filler 2 had a lower real part of the complex permeability and higher imaginary part

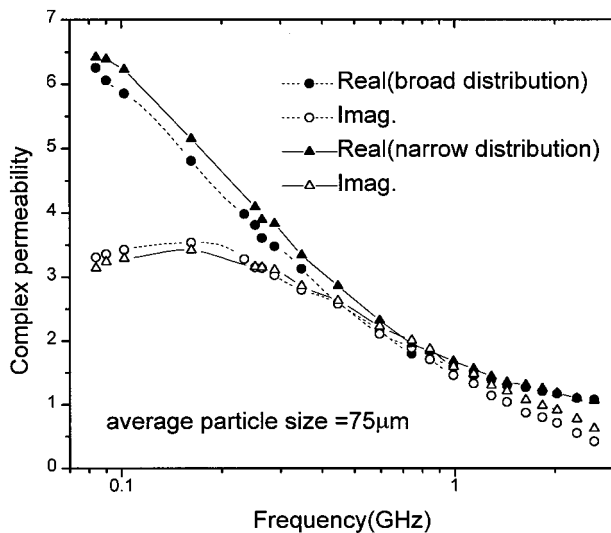


Figure 3 The dispersion spectra of complex permeability for the composite with different particle size distribution (ferrite volume fraction = 0.5).

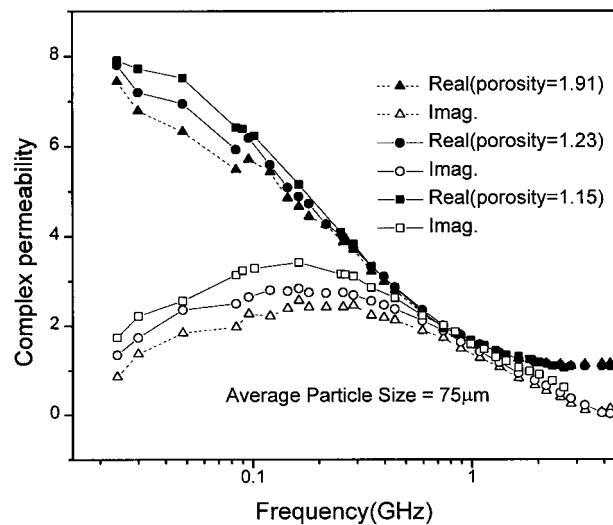


Figure 4 The effect of porosity on complex permeability of composite containing the ferrite of narrow particle size distribution.

than the composite with filler 1. In case of the broad particle size distribution like filler 1, it is believed that magnetic moment of a particle is superimposed with that of neighboring particles, so the dispersed rotational energy of a spin moment makes the real part of the complex permeability lower and the loss term of the permeability gets to be higher.

Figure 4 shows the effect of the complex permeability on porosity for the composite with filler 1. Below the relaxation frequency, at which the imaginary part of the complex permeability was maximal, both the real part and imaginary part decreased as the porosity increased, above that frequency the reversal behavior gradually occurred. The relaxation curve had flattened considerably as porosity increased. The reason is that the relaxation frequency has distribution, not a fixed value. The reason why the distribution of the relaxation frequency appears is that the rotational movement of a spin hindered by the porosity leads fluctuation of the respective relaxation frequencies of the phases in material.

Han et al.⁵ have proposed the model for the electromagnetic property on the ferrite-epoxy system using a rule of mixture. They described the effective permeability of the composite as follows:

$$\mu_{eo} = \frac{\mu_{io}(1 + X)}{(X\mu_{io} + 1)} \quad (1)$$

Here, μ_{eo} is the effective permeability of the composite, μ_{io} is the initial permeability of the sint-

ered ferrite, and X is $(1/V)^{1/3} - 1$, which is a function related to the ferrite content. V is the volume fraction of ferrite. Han⁶ has also proposed the relaxation behavior equation for the frequency dispersion characteristics of the complex permeability on the ferrite–epoxy composite as follows:

$$\mu_e' = \frac{\mu_{eo}}{1 + (f/f_{cr})^2} \quad (2a)$$

$$\mu_e'' = \frac{\mu_{eo}(f/f_{cr})}{1 + (f/f_{cr})^2} \quad (2b)$$

$$f_{cr} = \frac{f_o \mu_{io}(X + 1)}{\mu_{eo}} \quad (2c)$$

Here, f_o is the resonance frequency of the sintered ferrite, and f_{cr} is the relaxation frequency of a composite with the magnetic and nonmagnetic material.

Using Han's models 1 and 2 (eqs. 3a and 3b), the effective permeability and the relaxation frequency of the composite are relatively well predictable. However, the relaxation phenomena due to the interaction between the matrix and particle cannot be fully explained. This is due to many simplifications of the real composite, such as (1) an ideal mixing of the ferrite and epoxy, (2) single particle size, and (3) the composite was as a sintered phase with small permeability. Practically, however, the frequency dispersion behavior of a composite is very complicated because the rotational movement of a magnetic dipole in a given frequency is greatly affected by many factors, such as the ferrite content, particle size, porosity, and so on. Therefore, in this article, the frequency dispersion model of the complex permittivity was applied to the complex permeability, and then the factors related with the model were determined. From the frequency dispersion behavior of the complex permeability of the epoxy–ferrite composite, it was found that the imaginary part was asymmetrical to the relaxation frequency, and the loss term was greatly damped. Consequently Cole and Cole,⁷ Davidson and Cole,⁸ and Havriliak and Negami⁹ models established for the complex permittivity were modified for the complex permeability. The proposed models are as follows:

Model 1

$$\mu_e = \mu_\infty + \frac{\mu_{eo} - \mu_\infty}{1 + \left(\frac{f \mu_{eo}}{f_o \mu_{io}(X + 1)} \right)^{2(1-\sigma)}} \quad (3a)$$

Model 2

$$\mu_e = \mu_\infty + \frac{\mu_{eo} - \mu_\infty}{\left[1 + \left(\frac{f \mu_{eo}}{f_o \mu_{io}(X + 1)} \right)^2 \right]^\nu} \quad (3b)$$

Model 3

$$\mu_e = \mu_\infty + \frac{\mu_{eo} - \mu_\infty}{\left[1 + \left(\frac{f \mu_{eo}}{f_o \mu_{io}(X + 1)} \right)^{2(1-\sigma)} \right]^\nu} \quad (3c)$$

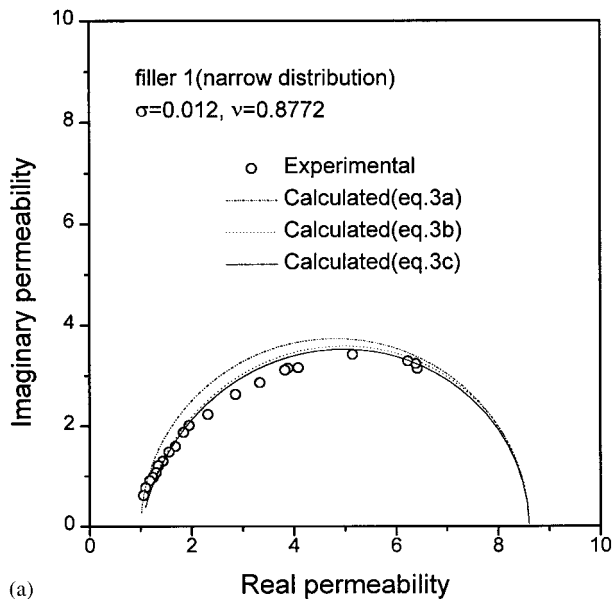
Here, σ and ν are a damping factor and an asymmetrical factor, respectively. The values range from 0 to 1. The permeability of the composite at an infinite frequency is μ_∞ , and will be ~ 1 , the permeability of pure epoxy.

Equation (3a) shows the ideal behavior at $\sigma = 0$, eq. (3b) at $\nu = 1$, and eq. (3c) at $\sigma = 0$ and $\nu = 1$. For the ideal case, a plot of the real versus imaginary parts will lead to a semicircle, whose center point is on the real axis in the complex permeability plane, but most materials do not exhibit ideal behavior. Equations (3a)–(3c) represent non-ideal behaviors. Equation (3a) exhibits a damping, that is, the center point of a semicircle is below the real axis. Equation (3a) describes the relaxation properties of the material that are symmetric about f_{cr} [eq. (2c)], the relaxation frequency. On the other hand, the eq. (3b) describes the relaxation properties of materials that are asymmetric about f_{cr} . Equation (3c) is a generation of the two equations above.

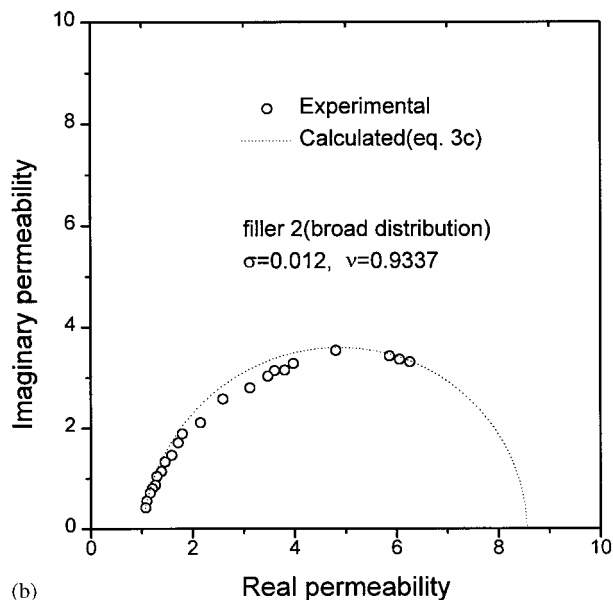
Figure 5(a) shows the comparison of calculated value of μ_e using eq. (3) with the experimental value for the filler–epoxy composite. As shown in this figure, eq. (3c) coincided with the experimental value fairly well. Hence, eq. (3c) enables the frequency dispersion behavior for the composite to be predicted. In this case, σ and ν were 0.012 and 0.872, respectively.

Figure 5(b) shows the imaginary and real part of the complex permeability of the composite with filler 2 obtained from the experimental data and the calculation using eq. (3c). The experimental data were well approximated to the calculation. The values of σ and ν of the filler were 0.012 and 0.9337, respectively. In Fig. 5(a) and (b), σ was the same value in both cases and the composite with filler 2 showed lower ν . The curve gets more asymmetrical as ν decreases.

In Figure 6 the composites, which have the same particle size distribution but different poros-



(a)



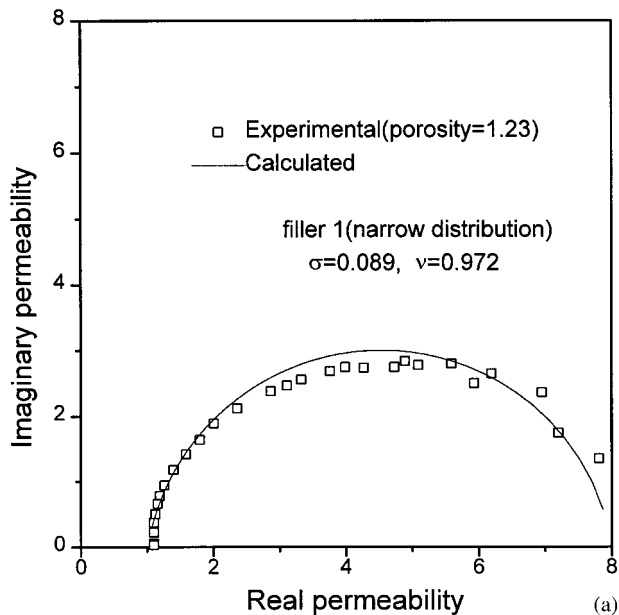
(b)

Figure 5 (a) Comparison of experimental values with calculated values in eq. (3); (b) comparison of experimental values with calculated values in eq. (3c).

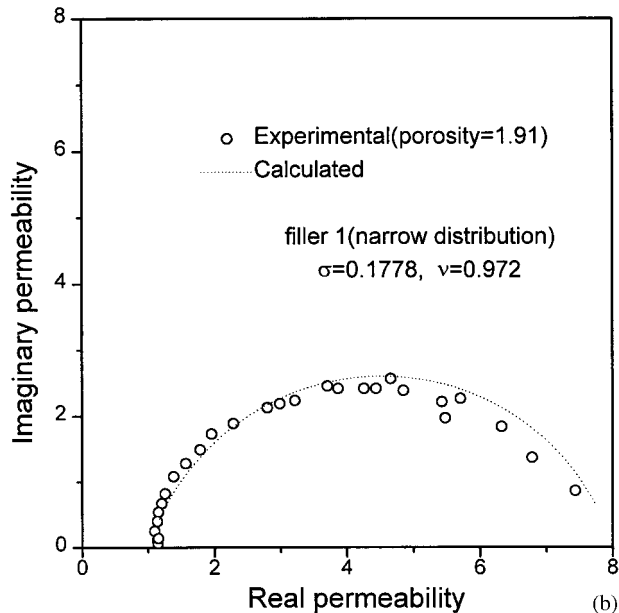
ity, were compared. The experimental value coincided well with the calculation. The value of σ varied from 0.089 to 0.1778 with the increase of porosity. From that result, it is found that the porosity of the composite changes the relaxation frequency range of the dispersion behavior curve and can affect the damping.

Figure 7(a,b) shows the relationship between the real and imaginary part of the complex permeability for the composite with the filler content of

0.5 volume fraction, whose particle size is 100 and 40 μm , respectively. The solid and dashed lines are calculated from eq. (3c) and the marks are experimentally obtained. They coincided well with each other. When the particle size is 100 μm , σ is 0.0788 and ν is 0.988. When the particle size is 40 μm , σ and ν are 0.122 and 0.9113, respec-



(a)



(b)

Figure 6 (a) Comparison of experimental values with calculated values for porosity in eq. (3c); (b) comparison of experimental values with calculated values for porosity in eq. (3c).

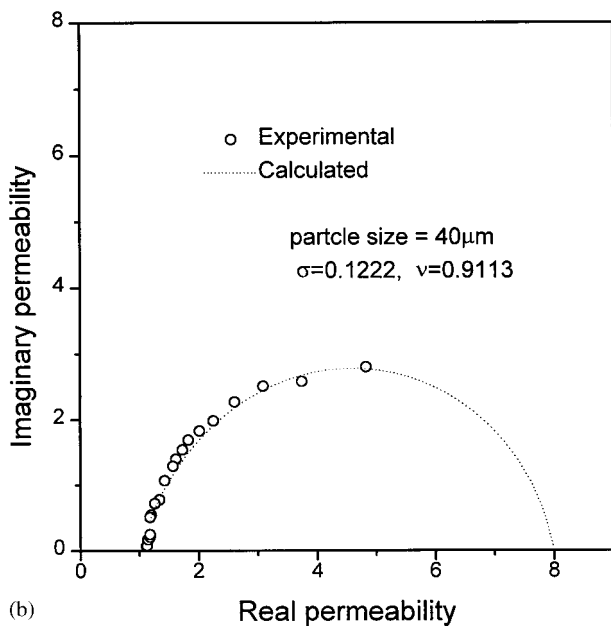
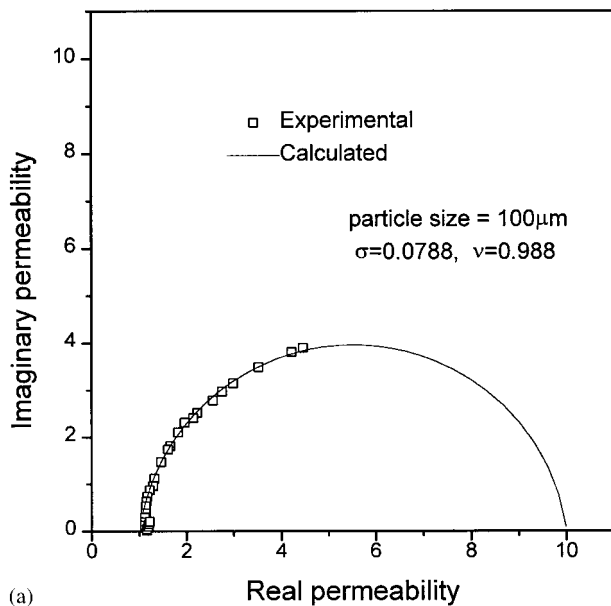


Figure 7 (a) Comparison of experimental values with calculated values for particle size in (3c); (b) comparison of experimental values with calculated values for particle size in eq. (3c).

tively. The damping factor is decreased with the increase of the particle size.

CONCLUSIONS

The complex permeability of the composite increased with the increase of ferrite particle size. The ferrite content and the porosity of the composite with the same particle size affect the frequency dispersion behavior. The relaxation curve flattened as the porosity increased.

Equation (3c) is a fair prediction of the frequency dispersion behavior of the complex permeability for the composite. The variation of σ and ν is related to the shape of the frequency dispersion curve. The center point of the Cole–Cole curve gradually moves down as σ increases, and finally the curve flattens. The curve becomes more asymmetrical with the increase of ν . It was found that σ and ν are the parameters related to the porosity, the particle size, and the particle size distribution.

REFERENCES

1. H. D. Choi, W. S. Kim, K. C. Han, K. Y. Kim, and T. J. Moon, *Polymer (Korea)*, **19**, 587 (1994).
2. H. D. Choi, W. S. Kim, I. S. Jeon, and T. J. Moon, *Polymer (Korea)*, **20**, 658 (1996).
3. Y. Naito and K. Suetake, *IEEE Trans. Micro. Theo. Tech.*, **19**, 65 (1971).
4. A. M. Nicolson and G. F. Ross, *IEEE Trans. Instrum. Meas.*, **19**, 377 (1970).
5. K. C. Han, H. D. Choi, T. J. Moon, W. S. Kim, and K. Y. Kim, *J. Mater. Sci.*, **30**, 3567 (1995).
6. K. C. Han, Ph.D. Thesis, Korea University, 1994.
7. K. S. Cole and R. H. Cole, *J. Chem. Phys.*, **9**, 341 (1941).
8. D. W. Davidson and R. H. Cole, *J. Chem. Phys.*, **18**, 1417 (1951).
9. S. Havriliak and S. Negami, *Polymer*, **8**, 161 (1967).